Cloud-Chamber Photographs at 4310 Meters Altitude

W. H. BOSTICK

Ryerson Physical Laboratory, University of Chicago, Chicago, Illinois

(Received December 1, 1941)

Cloud-chamber photographs taken at 4310 meters altitude give evidence for the existence of penetrating particles in air showers. Out of 2983 successful expansions 5.8 percent showed particles classified either as slow mesotrons or slow protons. 1.3 percent of the expansions show particles whose specific ionization increases markedly on passing through a 1.3-cm lead plate in the chamber. Twenty-seven photographs show penetrating pairs and thus indicate the production of penetrating secondaries at this altitude. Some photographs give evidence for nuclear processes associated with showers. Five photographs show electrons which may have come from the disintegration of mesotrons within the chamber.

IN connection with a cosmic-ray expedition sent from the University of Chicago to Mt. Evans in August, 1940, the author took a series of cloud-chamber photographs. It was hoped by these experiments to confirm the existence of penetrating particles believed from previous counter tube observations to be present in large air showers. It was also desired to obtain data on the number of heavily ionizing cosmic-ray particles and on the number of particles generated and stopped in a lead plate in the chamber.

The equipment consisted of a cloud chamber, counter controlled by any of the two-, three-, and fourfold coincidence arrangements of Geiger-Mueller counter tubes shown in Fig. 1 and indicated by the letters, A, B, $\cdots$ G. To aid in distinguishing particles of different types a lead plate 1.3 cm thick was placed in the middle of the chamber. With this procedure, some of the cosmic-ray particles can be identified on the basis of (a) the increase of ionization on passing through the lead plate, (b) the production of secondaries, and (c) the scattering of the particle in the lead plate.

The cloud chamber, 24 cm in diameter and 7 cm in illuminated depth, was used without magnetic field. The illumination was provided by four automobile headlight lamps, each having two 32-candle-power filaments. The lamps were mounted in parabolic reflectors and all the filaments were connected in series. Power for these lamps was provided by a 450-watt a.c. gasoline electric generator. The filaments were operated at a dull red except during expansions. The camera arrangement was stereoscopic. The counter circuit and cloud-chamber timing control

were those used by Herzog[1] and Herzog and Bostick.[2]

(1) PENETRATING PARTICLES IN AIR SHOWERS

The fourfold coincidence arrangements D and F in Fig. 1 were used to photograph particles in air showers penetrating, respectively, 12.7 and 20 cm of lead. For electrons that traverse the 1.3-cm lead plate, under the conditions of the experiment, there is a probability of from 3 to 22 percent that no multiplication will occur.[3] If, as is actually the case, a much larger fraction of the particles traverse without multiplication, we may infer the presence of mesotrons or protons. This fraction traversing without multiplication is seen from Table II to be, respectively, 93 and 86 percent of the total number of traversing particles observed in the photographs triggered by air showers. This demonstrates the presence of penetrating particles (mesotrons or protons) in air showers.
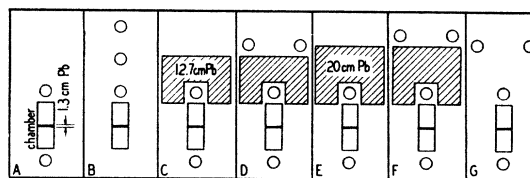
The investigations of Janossy and Ingleby,[4] and

FIG. 1. Arrangement of counters.

[1] G. Herzog, Phys. Rev. **59**, 117 (1941).
[2] G. Herzog and W. H. Bostick, Phys. Rev. **59**, 122 (1941).
[3] According to Arley's calculation [Proc. Roy. Soc. **A168**, 525 (1938)] 3 percent of the electrons of energy above 2×10^8 ev traversing the lead plate should emerge as single particles. For electrons under 2×10^8 ev, this calculated fraction is 22 percent.
[4] L. Janossy and P. Ingleby, Nature **145**, 511 (1940).

TABLE I. Data on cloud-chamber photographs.

Counter Arrangement		A	B	C	D	E	F	G	Totals
(1) Total number of photographs		653	1430	593	58	89	80	80	2983
(2) Number of particles penetrating the 1.3-cm lead plate in the chamber without producing any secondaries		210	330	252	13	38	12	4	859 (29%)
(3) Number of particles producing secondaries in the 1.3-cm lead plate (excluding those cases where a large shower was seen in the chamber)		24	55	25	1	5	2	4	116 (3.9%)
(4) Number of particles penetrating the 1.3-cm lead plate in pairs without producing any secondaries		6	24	18	2	2	2	4	54 (1.8%)
(5) Number of particles judged by their specific ionization and range to be	Angle with the vertical								
	slow mesotrons 0°–30°	21	25	4	5	3	6	3	67
	30°–60°	2	7	4	2	0	2	1	18
	60°–90°	3	3	3	0	0	0	0	9
	slow protons 0°–30°	5	18	8	1	1	2	0	35
	30°–60°	5	11	7	3	1	0	0	27
	60°–90°	5	6	0	3	1	0	1	16
(6) Number of particles showing marked increase in specific ionization on passing through 1.3 cm of lead in the chamber and their classification according to that appearance (see Figs. 8, 9, 10, and 11)	slow mesotrons	14	6	5	2	2	0	0	29
	slow protons	0	6	3	0	0	1	0	10
(7) Number of particles produced in 1.3 cm of lead in the chamber by non-ionizing radiation, judged by their specific ionization and range to be (see Fig. 12)	slow mesotrons	5	16	3	4	2	2	2	34
	slow protons	2	10	4	1	0	0	0	17
	fast particles	19	83	25	10	6	3	3	146
(8) Particles stopped in 1.3 cm of lead in the chamber judged by their specific ionization to be (see Fig. 9)	slow mesotrons	1	11	2	1	1	1	1	18
	slow protons	0	2	1	1	0	1	0	5
	fast particles	7	37	9	1	3	5	4	66
(9) Number of large showers with greater than 50 particles in the chamber (see Fig. 4)		1	1	3	3	0	2	1	11 (0.4%)

Totals with braces: (5) 172 (5.8%); (6) 39 (1.3%); (7) 51 (1.3%); (8) 23 (0.8%).

of Wataghin, Pompeia, and Santos[5] demonstrate the existence of cosmic-ray particles in showers at sea level capable of penetrating 50 and 63 cm of lead. If the extremely high penetration of these showers is to be interpreted by the cascade theory, these showers would have been initiated at the top of the atmosphere by single particles with the unbelievably high energy of 10^{19} ev. Swann and Ramsey[6] report pairs of particles penetrating 4 to 18 cm of lead without any apparent production of secondaries. Auger[7] and also Hilberry[8] find the number of extensive showers at low altitudes considerably greater than the number predicted by the cascade theory. Finally, Hilberry and Regener,[9] working with extensive showers at Mt. Evans, and Wataghin,[5] using counter arrangements separated by 11 and 30 cm of lead, show that the reduction in the number of showers by lead absorbers is far less than expected from the cascade theory. The same discrepancy is shown in the contrast between rows 11 and 13 of Table II in this paper. In order to explain these departures from the cascade theory all of the above mentioned investigators suggest, in accord with the evidence just presented, that penetrating particles are present in air showers.

A possible explanation for the presence of such particles in air showers was suggested by Booth and Wilson[10] and also by Christy and Kusaka[11] who calculated the pair production of spin 1 mesotrons by γ-rays and found that at energies greater than 10^{14} ev mesotron pair production is more probable than pair production of electrons.

TABLE II. Photographs showing penetrating particles taken with counter arrangements D and F of Fig. 1.

		D	F
(1)	Counter arrangement	D	F
(2)	Thickness of lead above the chamber	12.7 cm	20 cm
(3)	Number of photographs taken with four-fold shower triggering of Table I	58	80
(4)	Number of photographs in (3) with particles penetrating the 1.3-cm lead plate without multiplying	12	11
(5)	Ratio, Item (4)/Item (3)	21%	14%
(6)	Fraction of random expansions showing particles penetrating 1.3 cm of lead without multiplication	—	4.6±2.7%
(7)	Number of particles in (3) that penetrate the 1.3-cm lead plate without multiplication	13	12
(8)	Number of particles in (3) penetrating the 1.3 cm of lead with multiplication (excluding particles in showers of greater than 50 particles in the chamber)	1	2
(9)	The fractional number of particles in (3) penetrating without multiplication, i.e., (7)/[(7)+(8)]	93%	86%
(10)	The fractional number of electrons (calculated by Arley) which would penetrate the plate without multiplication	3%–22%	3%–22%
(11)	Item (4) per hour	0.43 ±0.12	0.42 ±0.12
(12)	Accidental fourfold shower triggerings per hour	0.02	0.02
(13)*	For purely cascade processes the relative numbers of showers penetrating the different thicknesses of lead to be expected in equal time intervals	1	10^{-4}
(14)	Number of photographs in (3) showing large showers (more than 50 particles in the chamber)	3	2

[5] G. W. Wataghin, M. D. Santos, and P. A. Pompeia, Phys. Rev. 57, 61 (1940); 57, 339 (1940); 59, 902 (1941).
[6] W. F. G. Swann and W. E. Ramsey, Phys. Rev. 57, 1051 (1940).
[7] P. Auger et al., Rev. Mod. Phys. 11, 289 (1939).
[8] N. Hilberry, Phys. Rev. 59, 763 (1941).
[9] N. Hilberry and V. H. Regener, Phys. Rev. 59, 471 (1941).

* This calculation uses curves plotted by N. Hilberry from Serber's calculations [Phys. Rev. 54, 317 (1938)] for the penetration of showers of a given energy, and a differential primary energy spectrum $dN = kE^{-2.9}dE$.

[10] F. Booth and A. H. Wilson, Proc. Roy. Soc. A175, 483 (1940).
[11] R. F. Christy and S. Kusaka, Phys. Rev. 59, 403 (1941).

However, it is very doubtful that the mesotron possesses spin 1, and for mesotrons of spin 0 or $\frac{1}{2}$ the predicted pair production is practically negligible even at the highest γ-ray energies.
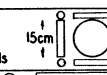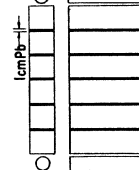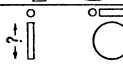
(2) ABUNDANCE OF HEAVILY IONIZING PARTICLES

The differentiation between a slow mesotron and a slow proton on the basis of measurements of range and estimates of ionization, though theoretically possible, is not very accurate. Nevertheless, some information can thus be obtained. The numbers of slow particles classified by this method are tabulated in Table I, row (5). The classification is divided according to the angles the tracks make with the vertical. The number of slow particles showing tracks with angles less than 30° with the vertical predominates for both mesotrons and protons. This leads to the belief that some of the slow protons and a large proportion of the slow mesotrons are produced not in nuclear evaporations, which would certainly give a more uniform angular distribution of the heavy particles than observed, but in events in which the vertical direction predominates.

Several investigators have obtained photographs of heavily ionizing cosmic-ray particles at various altitudes. A brief summary of their work is given in Table III. These results show a very marked increase in the number of heavily ionizing particles with height above sea level. As can be seen from Table I, row (5), the author obtained such tracks in 5.8 percent of the photographs taken at Mt. Evans, thus confirming these earlier results.

(3) CLASSIFICATION OF PARTICLES SHOWING AN INCREASE IN SPECIFIC IONIZATION ON PASSING THROUGH THE LEAD PLATE

(a) A marked increase in ionization on passing through the 1.3-cm lead plate in the chamber was observed for 39 tracks (see Table I, row (6), and Figs. 8, 9, 10, and 11). These particles were classified as mesotrons or protons according to the curves A and B in Fig. 2, which show the expected increases in ionization for mesotrons and protons of various incident kinetic energies as they traverse the lead plate. These curves in Fig. 2 were calculated from the range curves for mesotrons and protons in lead (see Fig. 3, curves

TABLE III. Summary of photographs of heavily ionizing particles.

AUTHOR CLOUD CHAMBER	ALTITUDE OF OBSERVATIONS	NUMBER OF EXPANSIONS	NO. OF SLOW MESOTRONS	NO. OF SLOW PROTONS	TOTAL NO. OF TRACKS WITH IONIZATION>FAST e'S	NO. OF EXPANSIONS / TOTAL NO. OF HEAVY TRACKS
Anderson[1] H = 7900 oersteds	14,000 ft	9188			123	1 in 75
	sea level					1 in 885
Powell[2] H = 0	14000 ft					1 in 80
Herzog[3] H = 708	15,000 to 29,000 ft	155	39	51	90	1 in 1.7
	10,000 to 15,000 ft	29	0	3	3	1 in 10
Brode[4] H = 0	sea level	8500		21	80	1 in 106
Auger[5] H = ?	10,000 ft	with ordinary shower control				1 in 75
		with extensive shower control				1 in 8
Johnson[6] H = 0	sea level	4000		3	3	1 in 1300
Bostick H = 0	14000 ft	2983	94	78	172	1 in 18

[1] C. D. Anderson and S. H. Neddermeyer, Phys. Rev. 50, 263 (1936).
[2] W. Powell, Phys. Rev. 58, 474 (1940).
[3] G. Herzog, Phys. Rev. 59, 117 (1941).
[4] R. B. Brode, Phys. Rev. 50, 587 (1936).
[5] P. Auger, Rev. Mod. Phys. 11, 289 (1939).
[6] T. H. Johnson, Barry, and Shutt, Phys. Rev. 57, 1047 (1940).

5 and 6) and from the energy loss by ionization curves in argon, the gas in the chamber. The former were obtained by graphical integration of the Bloch formula for energy loss by ionization.* Figure 2 shows that a 10^8 ev proton entering the lead plate should exhibit an ionization in argon of 3.7 (curve A_P) in the units used in Fig. 2, and after traversing the plate should exhibit an ionization of 9.5 (curve B_P), which respresents an increase by a factor of 2.6. On the other hand, a mesotron which traverses the lead plate and exhibits an increase in ionization by a factor of 2.6, should enter with an ionization of only 1.55
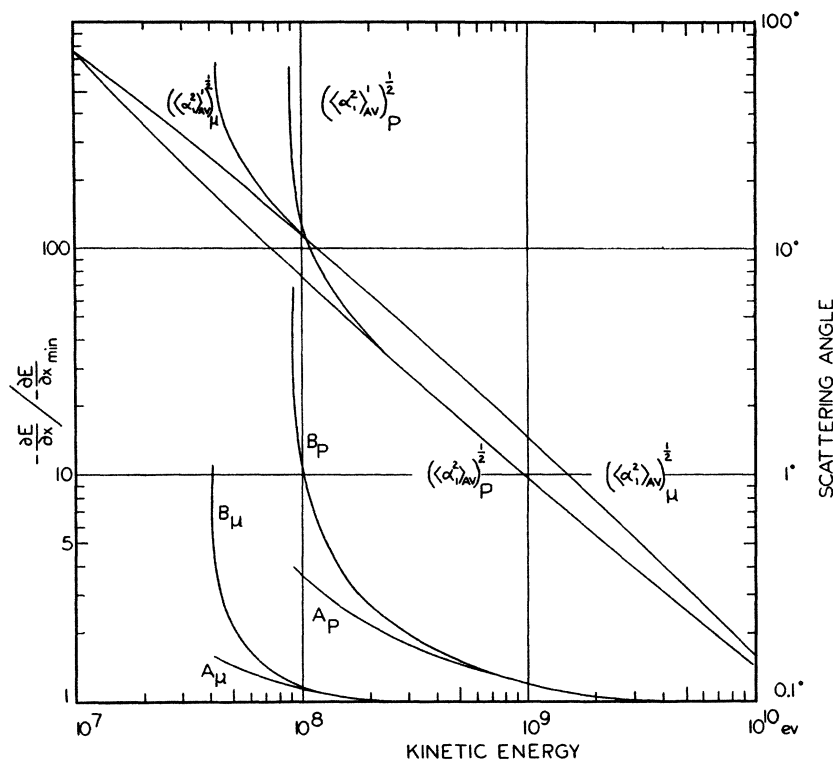
* See Appendix A.

FIG. 2. The specific ionization in argon is expressed in terms of the minimum ionization that a particle can experience in argon. μ refers to a mesotron of mass $200m_e$ and P to a proton of mass $1840m_e$. A_μ is the specific ionization in argon by a mesotron entering the lead plate vs. its kinetic energy. B_μ is the specific ionization in argon by a mesotron as it leaves the lead plate vs. the kinetic energy it possessed *when it entered*. A_P and B_P are the corresponding curves for protons. $(\langle \alpha_1^2 \rangle_{Av})_\mu^{\frac{1}{2}}$ is the root mean square scattering angle of a mesotron calculated from Williams (see Appendix B) for a finite nucleus and shielding, for 1.3 cm of lead, neglecting the loss of energy by ionization in the lead plate. $(\langle \alpha_1^2 \rangle_{Av})_P^{\frac{1}{2}}$ is the corresponding curve for a proton. $(\langle \alpha_1^2 \rangle_{Av}^1)_\mu^{\frac{1}{2}}$ is the root mean square scattering angle for a mesotron after energy loss in the plate has been considered. $(\langle \alpha_1^2 \rangle_{Av}^1)_P^{\frac{1}{2}}$ is the corresponding curve for a proton.

(curve A_μ), and is thereby distinguishable from a proton. Finally, if a mesotron enters the lead plate with an ionization any higher than 1.56 it should stop in the lead plate. With this method, of the 39 tracks classified in row (6) of Table I, 29 were found to be slow mesotrons and 10 to be slow protons.

(b) Some of the 39 particles show a definite scattering in the lead plate. According to the theory of multiple scattering the mean scattering angle is a function of the kinetic energy. For the purposes of calculation this mean scattering angle was identified with the observed scattering angle, and the kinetic energies of the incident particles, assumed in turn to be mesotrons and protons, were computed.** Using this value of the kinetic

** See Appendix B.

energy of the incident particle, one can read from the curves A and B in Fig. 2 the expected increase in ionization as the particle passes through the lead plate. If the particles are assumed to be mesotrons, the expected increases of ionization thus calculated are not high enough to agree with the observed increases in any of the 39 tracks. On the other hand, if the particles are assumed to be protons, the expected increases of ionization are of the right order of magnitude i.e., from a comparison of the increase in ionization with the scattering angle all 39 particles are identified as protons.

Although for protons the calculated increase of ionization is thus of the right order of magnitude, the calculated density of ionization by the protons as they enter the lead plate is in most
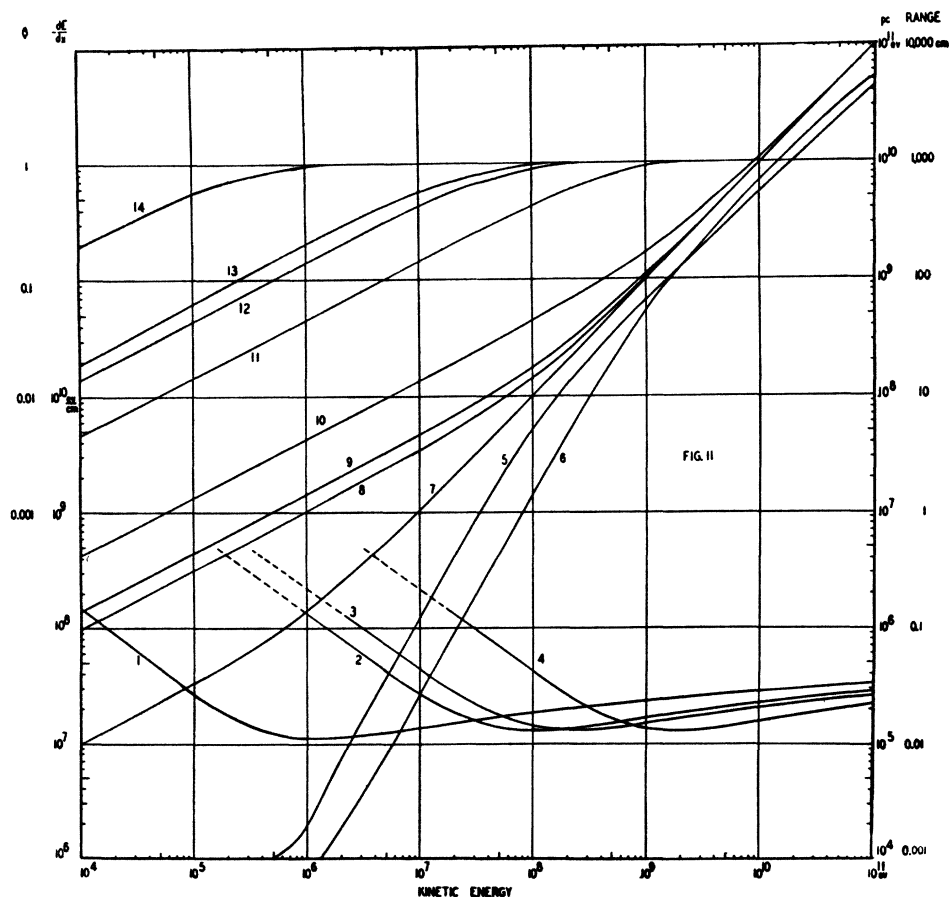
FIG. 3. Energy loss per cm by ionization is $-\partial E/\partial x$, pc is the momentum multiplied by c, β is v/c. $-\partial E/\partial x$ in lead vs. kinetic energy (1) for an electron; (2) for a mesotron of mass $100m_e$; (3) for a mesotron of mass $200m_e$; (4) for a proton of mass $1840m_e$.

Range in lead vs. kinetic energy (5) for a mesotron of mass $200m_e$; (6) for a proton of mass $1840m_e$. pc vs. kinetic energy (7) for an electron; (8) for a mesotron of mass $100m_e$; (9) for a mesotron of mass $200m_e$; (10) for a proton.

β vs. kinetic energy (11) for a proton; (12) for a mesotron of mass $200m_e$; (13) for a mesotron of mass $100m_e$; (14) for an electron.

cases three times higher than the observed value. This indicates that the identification of these particles as protons by using the scattering angle and increase of ionization as criteria is doubtful. Since the kinetic energy was not measured by a direct method (such as deflection in a magnetic field), but was calculated in case (a) from the theory of ionization loss, and in case (b) from the combination of ionization increase and the theory of multiple scattering, both methods have limitations in identifying heavily ionizing particles in cloud chambers. The difference in the classification of the particles by the two methods may thus merely reflect the uncertainty in the estimates of the density of ionization.

(4) PAIRS OF PENETRATING PARTICLES

Row (4) of Table I shows twenty-seven cases in which pairs of particles penetrated the 1.3-cm lead plate without producing secondaries.[12,13] In Fig. 5 a group of particles coming from the top (left) strike the plate, and two of them penetrate without multiplying. In Fig. 12 can be found a similar pair. All twenty-seven photographs show that penetrating particles can be produced in pairs or groups.

[12] H. J. J. Braddick and G. S. Hensby, Nature 144, 1012 (1939), publish a photograph of a penetrating pair taken at sea level.
[13] W. Powell, Phys. Rev. 58, 474 (1940), publishes a photograph of a penetrating pair obtained at Mt. Evans.

FIG. 4
FIG. 5
FIG. 6
FIG. 7
FIG. 8
FIG. 9
FIG. 10
FIG. 11
FIG. 12
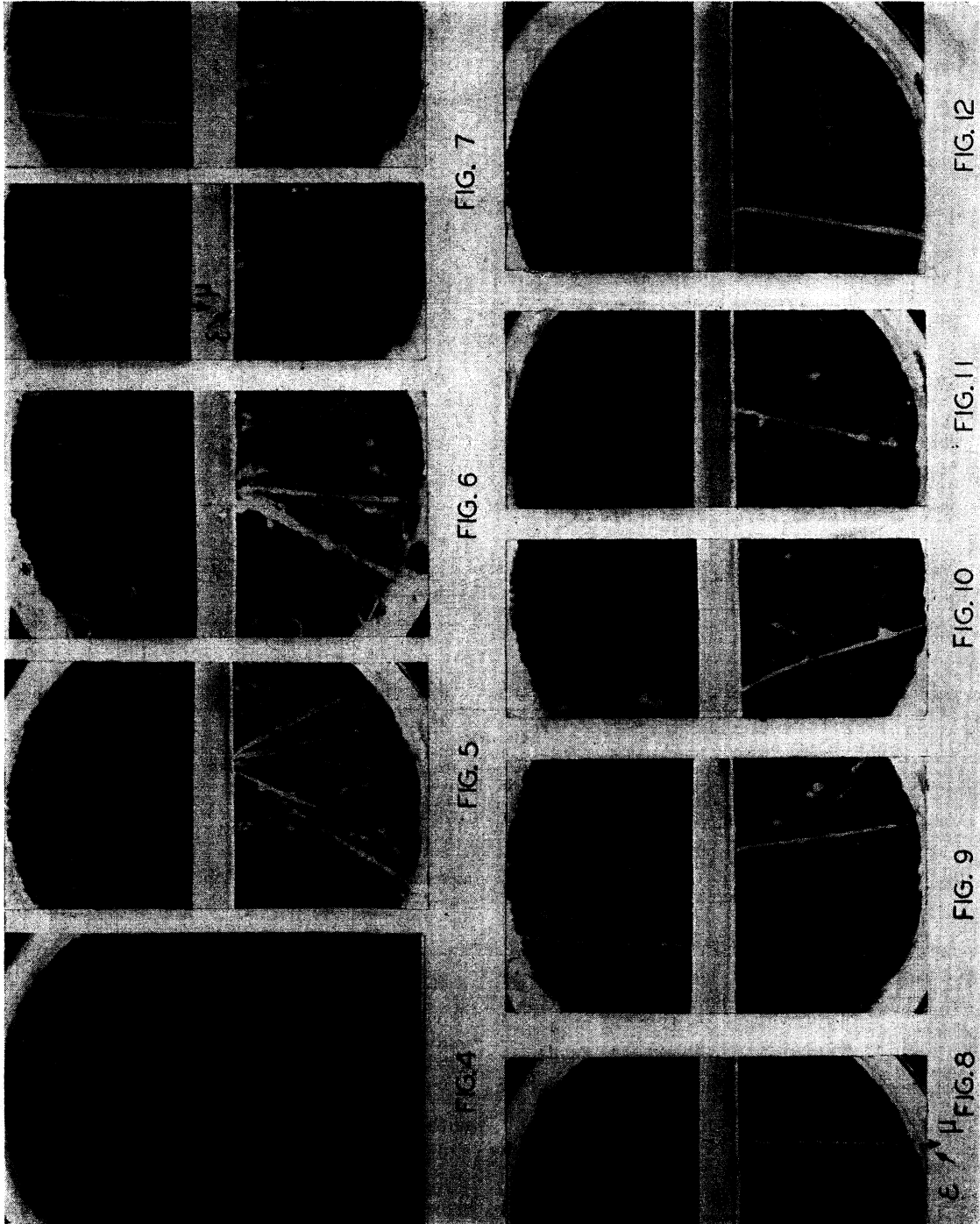
CAPTIONS TO FIGURES ON OPPOSITE PAGE

Figure 4, triggered by the fourfold coincidence arrangement F in Fig. 1 with 20 cm of lead above the chamber, shows a large shower in the chamber.

Figures 5 and 6 taken with no lead above the chamber show showers containing particles with specific ionization high enough to be either slow mesotrons or slow protons. Figure 5 shows at least 2 particles passing obliquely through the 1.3-cm lead plate without producing secondaries. It is, therefore, probable that these particles are not electrons, but are a shower of mesotrons or protons.

Figure 7, the two stereoscopic views show a particle with the specific ionization of a slow mesotron or a slow proton entering the plate and a particle with the specific ionization of a fast electron coming out below at an angle of 40° with the direction of the first track. A possible interpretation is that a slow mesotron disintegrates and gives rise to the electron below.

Figure 8 was taken with 12.7 cm of lead above the chamber and was triggered with the fourfold shower arrangement shown in D, Fig. 1. It shows a particle with the appearance of a fast mesotron markedly increasing its ionization on passing through 1.3 cm of lead, and according to the curves A_μ and B_μ in Fig. 2 it is classified as a mesotron. It is possible that the track in the bottom of the chamber is the decay electron of the slow mesotron.

Figures 9, 10, and 11 are examples of tracks showing a marked increase in specific ionization on passing through the lead plate. Figures 9 and 10 were taken with 12.7 cm of lead above the chamber, Fig. 11 with no lead above the chamber.

Figure 12, taken with arrangement B, Fig. 1, shows the following events occurring in the same expansion: (a) Shower production in the lead plate by an electron, (b) shower production in the lead plate by a photon, (c) a pair of particles penetrating the lead plate without multiplication, and (d) the production in the lead plate of a heavy particle by non-ionizing radiation. This heavy particle with its delta-rays is very similar in appearance to a heavy particle photographed by Herzog[1] at 8,800 meters.

(5) HEAVILY IONIZING PARTICLES ASSOCIATED WITH SHOWERS

Figure 12 shows the photograph of a heavy particle produced in the lead plate by non-ionizing radiation. This occurs simultaneously with a cascade shower in the chamber. The heavy particle with its accompanying delta-rays is very similar in appearance to that photographed by Herzog[1] at 8,800 meters altitude. Other cases of the simultaneous occurrence of heavily ionizing particles and cascade showers are reproduced in Figs. 5 and 6. These photographs agree with Korff's[14] conclusions that protons (and also neutrons) can be produced by a process connected with the soft component.

(6) POSSIBLE CASES OF MESOTRON DECAY

In Figs. 7 and 8 are reproduced two of the five photographs which might be explained by a spontaneous decay of the mesotron. In four of these

[14] S. A. Korff, Phys. Rev. 59, 949 (1941).

five photographs the particle assumed to be a decay electron originates from the stopping of a heavily ionizing particle in the lead plate (Fig. 7). Row (8) of Table I shows that 23 heavily ionizing particles and 66 particles with normal ionization were observed to stop in the lead plate. If all of these particles were mesotrons, we should expect more than the four observed disintegrations. The same infrequency of decay electrons was reported by Herzog and Bostick[2] where a 0.3-cm copper plate was placed in the middle of a cloud chamber carried to an altitude of 8,800 meters. Such results indicate that many of the heavily ionizing particles are protons, and that most of those of normal ionization which stop in the lead plate are electrons.

APPENDIX A

The Bloch[15,16] formula for the energy loss per cm of a charged particle by ionization processes in passing through a substance of atomic number Z is

$$-\frac{\partial E}{\partial x} = 2\pi\sigma Z r_0^2 \frac{m_e c^2}{\beta^2}\left[\log_e \frac{m_e c^2 \beta^2 W_m}{(1-\beta^2)I^2 Z^2}+1-\beta^2\right]$$

where σ is the number of atoms per cc, $r_0 = e^2/m_e c^2$, m_e is the mass of the electron, $\beta = v/c$, I is the mean ionization energy and is equal to 13.5 ev, e is the electronic charge, W_m is the maximum energy that can be imparted to an electron by a particle of Mass M.

$$\frac{W_m}{E_0 - Mc^2} = \frac{2m_e M(\gamma+1)}{m_e^2 + M^2 + 2m_e M\gamma},$$

where $E_0 - Mc^2$ is the kinetic energy, M is the rest mass of the incident particle and $\gamma = (1-\beta^2)^{-\frac{1}{2}}$.

The quantity $-\partial E/\partial x$ for lead can be plotted vs. kinetic energy for particles of mass m_e, $100m_e$, $200m_e$, and $1840m_e$ as has been done in Fig. 3. When these curves are drawn it is possible to obtain the range of the particles as a function of their kinetic energies by a graphical integration as shown in Table IV.

APPENDIX B

E. J. Williams[17] has calculated $(\langle \alpha_1^2 \rangle_{Av})^{\frac{1}{2}}$, the root mean square of the scattering angle, for a charged particle of

[15] F. Bloch, Ann. d. Physik 16, 285 (1933).
[16] H. J. Bhabha, Proc. Roy. Soc. A164, 270 (1938).
[17] E. J. Williams, Proc. Roy. Soc. A169, 531 (1938–39).

TABLE IV. Distance $d = (K_i - K_f)/-\langle\partial E/\partial x\rangle_{Av}$ is that traveled in lead when a particle of mass $200m_e$ and of an initial kinetic energy K_i loses by ionization an amount of energy equal to $K_i - K_f$, where K_f is the kinetic energy which the particle possesses after having traversed d. The average ionization loss per cm $-\langle\partial E/\partial x\rangle_{Av}$ is read from the curves in Fig. 3. The sum of the d's gives the range for a given K_i.

K_i (in ev)	K_f (in ev)	Av. $-(\partial E/\partial x)_{Av}$ (in ev/cm)	d (in cm)	Range (in cm)
10^4	0	10^{10}	10^{-6}	10^{-6}
10^5	10^4	5.0×10^9	1.8×10^{-5}	$10^{-6} + 1.8 \times 10^{-5} = 1.9 \times 10^{-5}$
5×10^5	10^5	5.0×10^8	10^{-2}	1.02×10^{-2}
10^6	5×10^5	2.7×10^8	1.85×10^{-3}	2.87×10^{-2}
5×10^6	10^6	1.14×10^8	3.54×10^{-2}	3.83×10^{-2}
10^7	5×10^6	5.85×10^7	8.55×10^{-2}	0.125
2×10^7	10^7	3.41×10^7	0.294	0.419

mass M, where $\langle\alpha_1^2\rangle_{Av} + \langle\alpha_2^2\rangle_{Av} = \langle\theta^2\rangle_{Av}$ and θ is the total scattering angle, and α_1 and α_2 are the scattering angles projected in two perpendicular planes, each of which contains the track of the incident particle. Neglecting the energy loss by ionization in the scattering material, taking into consideration shielding by electrons, and using a finite nucleus with a radius of 10^{-12} cm, Williams obtains

the following expression:

$$(\langle\alpha_1^2\rangle_{Av})^{\frac{1}{2}} = \left(\frac{\pi}{2}\right)^{\frac{1}{4}} [19.5 - 3.1 \log_{10} Z]^{\frac{1}{2}} \frac{2(Nt)^{\frac{1}{2}} Ze^2 (1-\beta^2)^{\frac{1}{2}}}{Mc^2\beta^2},$$

where W is the atomic weight, Z is the atomic number, t is the thickness, and N is the number of atoms per cc of the scattering material, and e is the electronic charge. The values of $(\langle\alpha_1^2\rangle_{Av})^{\frac{1}{2}}$ vs. the kinetic energy for both mesotrons and protons are plotted in Fig. 1.

It is now desired to calculate the corresponding values of $(\langle\alpha_1^2\rangle_{Av})^{\frac{1}{2}}$ when the energy loss in the plate is taken into account. Consider a particle of mass $200m_e$ entering the 1.3-cm lead plate with a kinetic energy of 8×10^7 ev. It will be seen from curve 5 of Fig. 3 that this particle will emerge with a kinetic energy of 6.1×10^7 ev. For the average between the energies 8×10^7 and 6.1×10^7 ev, the scattering angle $(\langle\alpha_1^2\rangle_{Av})^{\frac{1}{2}}$ was read from the curve in Fig. 2. If this value of $(\langle\alpha_1^2\rangle_{Av})^{\frac{1}{2}}$ is now plotted against the incident kinetic energy of 8×10^7, we obtain a point on the curve for $(\langle\alpha_1^2\rangle_{Av}')^{\frac{1}{2}}$. For lower kinetic energies the averaging process was made more precise by dividing the plate up into thin sections, numbered $a, b, c, \cdots$, and calculating the average kinetic energy of the particle in each section and in turn the resulting $(\langle\alpha_1^2\rangle_{Av}')^{\frac{1}{2}}$ in each section. The total $(\langle\alpha_1^2\rangle_{Av}')^{\frac{1}{2}}$ for the 1.3 cm of lead is given by

$$(\langle\alpha_1^2\rangle_{Av}')^{\frac{1}{2}} = [\langle\alpha_a^2\rangle_{Av} + \langle\alpha_b^2\rangle_{Av} + \langle\alpha_c^2\rangle_{Av} + \cdots]^{\frac{1}{2}}.$$

Radioactive Isotopes of Praseodymium

J. W. DeWire,* M. L. Pool, AND J. D. Kurbatov
The Ohio State University, Columbus, Ohio
(Received March 3, 1942)

New nuclear reactions $Pr^{141}(dp)$, $Ce^{142}(pn)$, and $La^{139}(\alpha n)$ yielding radioactive isotope Pr^{142} have been observed. The decay curves obtained for Pr^{142} after chemical purifications showed a half-life of 19.3 ± 0.1 hours, a value considered to be more exact than that previously reported. The negative beta-ray spectrum was measured with a recently constructed magnetic spectrometer of the $180°$ focusing type and was found to have an end point of 2.14 ± 0.02 Mev. A weak gamma-ray approximately 1.9 Mev was found associated with this period. The isotope Pr^{140} has been formed by the reaction: $Pr^{141}(n,2\ n)$. Its half-life was measured as 3.4 ± 0.1 minutes. Cloud-chamber measurements yield an upper limit of 2.40 ± 0.15 Mev for its positron spectrum.

I. INTRODUCTION

THE study of radioactivity in praseodymium began with the work of Fermi and coworkers, who produced periods of 5 minutes and 19 hours by bombarding praseodymium with neutrons.[1] They reported that the 19-hour period was sensitive to water and found a half-value thickness for its beta-rays of 0.12 g/cm² of aluminum. Marsh and Sugden[2] assigned the

19-hour period to Pr^{142}, and Pool and Quill[3] found that the shorter period was a 3.5-minute positron emitter and assigned it to Pr^{140}. Recently these assignments were confirmed by Wu and Segrè,[4] who reported that the half-life of Pr^{142} was 18.7 hours. They found that this isotope emitted only electrons with a continuous spectrum having an upper limit of 2 Mev.

1 E. Fermi et al., Proc. Roy. Soc. 149, 522 (1935).
2 J. K. Marsh and S. Sugden, Nature 136, 102 (1935).
3 M. L. Pool and L. L. Quill, Phys. Rev. 53, 437 (1938).
4 C. S. Wu and E. Segrè, Phys. Rev. 61, 203 (1942).

FIG. 4   FIG. 5   FIG. 6   FIG. 7

$\varepsilon \nearrow \mu$ FIG. 8   FIG. 9   FIG. 10   FIG. 11   FIG. 12
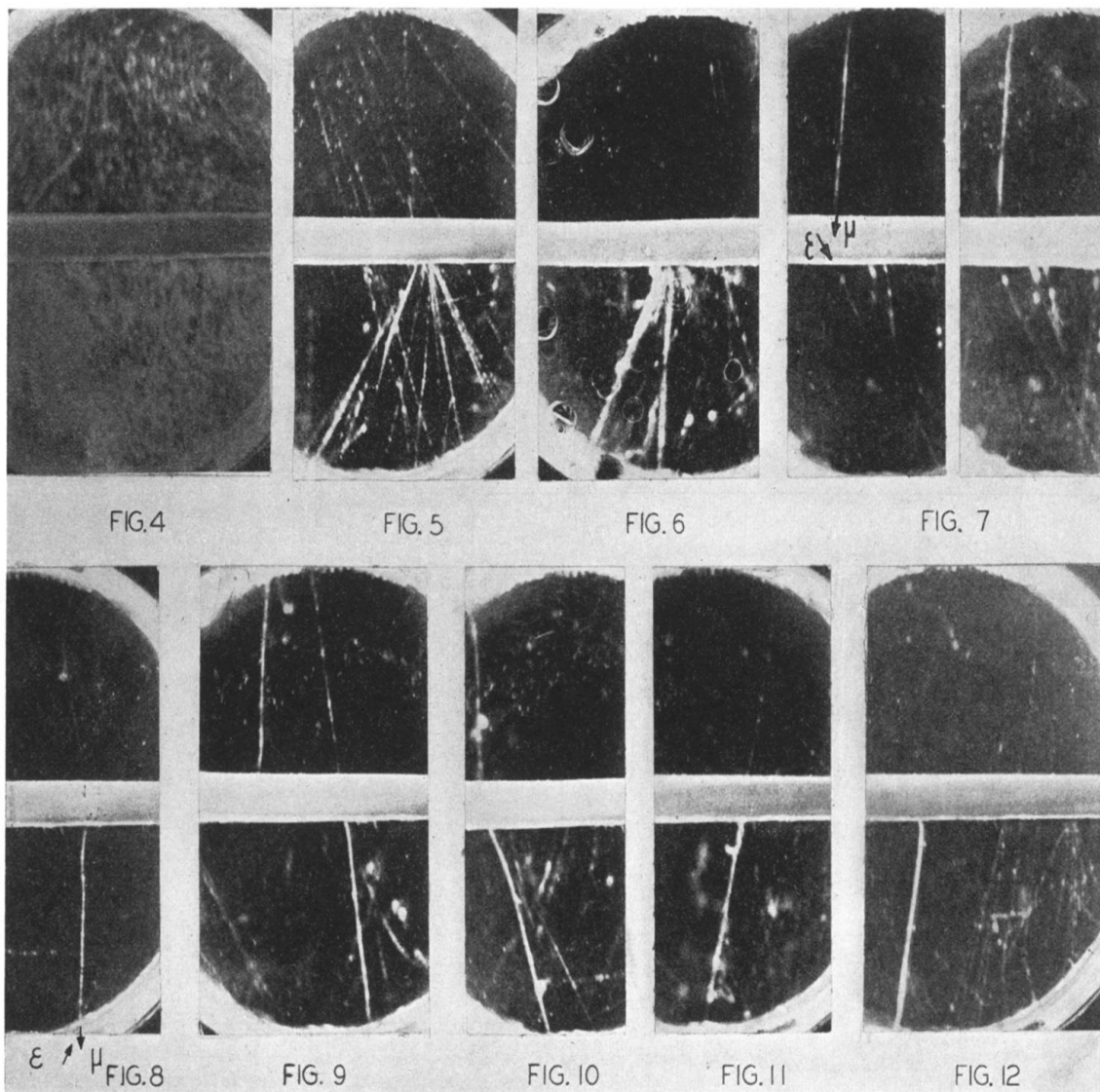
Figure 4, triggered by the fourfold coincidence arrangement F in Fig. 1 with 20 cm of lead above the chamber, shows a large shower in the chamber.

Figures 5 and 6 taken with no lead above the chamber show showers containing particles with specific ionization high enough to be either slow mesotrons or slow protons. Figure 5 shows at least 2 particles passing obliquely through the 1.3-cm lead plate without producing secondaries. It is, therefore, probable that these particles are not electrons, but are a shower of mesotrons or protons.

Figure 7, the two stereoscopic views show a particle with the specific ionization of a slow mesotron or a slow proton entering the plate and a particle with the specific ionization of a fast electron coming out below at an angle of 40° with the direction of the first track. A possible interpretation is that a slow mesotron disintegrates and gives rise to the electron below.

Figure 8 was taken with 12.7 cm of lead above the chamber and was triggered with the fourfold shower arrangement shown in D, Fig. 1. It shows a particle with the appearance of a fast mesotron markedly increasing its ionization on passing through 1.3 cm of lead, and according to the curves A_μ and B_μ in Fig. 2 it is classified as a mesotron. It is possible that the track in the bottom of the chamber is the decay electron of the slow mesotron.

Figures 9, 10, and 11 are examples of tracks showing a marked increase in specific ionization on passing through the lead plate. Figures 9 and 10 were taken with 12.7 cm of lead above the chamber, Fig. 11 with no lead above the chamber.

Figure 12, taken with arrangement B, Fig. 1, shows the following events occurring in the same expansion: (a) Shower production in the lead plate by an electron, (b) shower production in the lead plate by a photon, (c) a pair of particles penetrating the lead plate without multiplication, and (d) the production in the lead plate of a heavy particle by non-ionizing radiation. This heavy particle with its delta-rays is very similar in appearance to a heavy particle photographed by Herzog[1] at 8,800 meters.